J|A|C|S
COMMUNICATIONS

Published on Web 05/16/2007

Molecular Insight into the Pathway to Crystallization of Aluminum

Caroline Desgranges and Jerome Delhommelle*

Department of Chemical Engineering, 301 Main Street South, University of South Carolina, Columbia, South Carolina 29201

Received March 31, 2007; E-mail: delhomm@engr.sc.edu

Controlling the crystallization of metals is of key importance for many applications, such as metallic nanoparticles and catalysts. However, a complete understanding of this phenomenon still eludes us. Do metals crystallize according to the same mechanism as simple fluids? How do the strong cohesive interactions in metals affect the polymorph selection and the crystal morphology? In this communication, we simulate the entire crystallization process for aluminum at ambient pressure and at a temperature 20% below the melting point. We shed light on the molecular mechanisms underlying the crystal nucleation and growth of Al. We show that Al nucleates into a random packing of the hexagonal close-packed (hcp) and the face-centered cubic (fcc) phases. Body-centered cubic (bcc) clusters, which usually form during the nucleation of simple fluids (e.g., hard spheres,[1] Lennard-Jones,[2,3] and charge-stabilized colloids[4]), are not observed during the crystallization of Al. Throughout nucleation and growth, Al nuclei are always strongly faceted. This is in sharp contrast with the ellipsoidal crystallites observed during the crystallization of simple fluids.[1−5] Our results demonstrate that the pathway to crystallization of Al strongly departs from that of a simple fluid.

The strong cohesive interactions in metals are often described with an embedded-atoms model (EAM) potential.[6] In this work, we choose the EAM model parametrized by Jasper et al. (noted NP-B in their publication[7]). This many-body potential was validated against density functional theory results for Al clusters and nanoparticles. The ability of the model to accurately predict thermodynamics properties (e.g., boiling and melting points at ambient pressure as well as the solid densities for the stable fcc phase) was recently established.[8,9]

We study the onset of crystallization in a supercooled liquid of Al at $P = 1$ atm and at $T = 897.6$ K (20% below the melting temperature[9]). We carry out two different types of hybrid Monte Carlo (HMC) simulations corresponding to the two mechanistic steps of crystal growth and nucleation. We first induce the formation of a critical nucleus. To study this activated process, we perform a series of HMC simulations,[10] together with an umbrella sampling bias potential, on systems of 3000 Al atoms. The bias potential essentially imposes a fixed value of the global order parameter[11] Q_6 to the system and allows the system to overcome the free energy barrier of nucleation.[2] By gradually increasing the imposed value for Q_6, we are able to grow a crystal nucleus. This procedure does not favor the formation of a specific polymorph since Q_6 takes similar values for the fcc, hcp, and bcc polymorphs. As shown in previous work on charge-stabilized colloidal suspensions,[4] this method led to the formation of large fcc or bcc crystallites, whichever was the stable form for the conditions of crystallization investigated. Using local bond order parameters,[2,3] we analyze the structure of the nucleus throughout nucleation. We find that Al directly nucleates into a random packing of two phases, which are structurally compatible and have almost equivalent free energies: the stable fcc phase and the hcp phase. The critical nucleus contains 225 ± 32 particles and consists almost exclusively of a random packing of mainly fcc and hcp atoms ($92 \pm 8\%$ of the atoms are identified as fcc or hcp). Figure 1 shows a snapshot of a critical nucleus (the free energy barrier of nucleation is of $21 \pm 2\ k_BT$). The structural identity of the critical nucleus is similar to that observed in simulations of crystal nucleation of hard spheres[1] and in experiments on concentrated colloidal suspensions.[5] However, there are two significant differences. Previous work shows that crystal nucleation[2,3] in simple fluids first proceeds in the metastable bcc phase and then converts into the stable fcc phase, in accord with Ostwald's step rule. Our results demonstrate that, in the case of Al, the number of bcc particles remains negligible throughout the nucleation step. Moreover, experiments[5] and simulations[1−3] show that, in simple fluids, the average shape of the critical nucleus is ellipsoidal with rough interfaces (e.g., "wetted" by bcc particles for the Lennard-Jones (LJ) system[2,3]). Our simulations reveal that Al nuclei are strongly faceted.

What is the cause of the discrepancy between the nucleation mechanisms? There are several features common to Al and simple fluids. Fcc is the stable polymorph for both. Besides, theoretical predictions argue that bcc clusters should easily form from supercooled liquids of spherical particles.[12,13] There is, however, a major difference between Al and simple fluids. The strong cohesive interactions in Al result in a very small difference between the solid and liquid densities. For Al, the fcc phase is only 5% denser than the liquid, while for the LJ system studied in refs 2 and 3, the fcc phase is denser by 11%. In supercooled Al liquid, a small density fluctuation will yield the more energetically favorable fcc, hcp, and icosahedral structures[14] rather than a bcc cluster. On the other hand, because of the larger difference between the solid and liquid densities, bcc is a more viable intermediate for the LJ system. We add that, throughout the nucleation step, the concentration of Al atoms, identified as icosahedral, in the liquid stays around 7% and that virtually no solid particles are identified as icosahedral. This indicates that icosahedral structures do not play an active role in the nucleation process.

Once we have formed the critical nucleus, we study its evolution in the absence of the bias potential by (i) embedding the system of 3000 particles containing a critical nucleus in a supercooled liquid of 27 000 particles, (ii) equilibrating the new system of 30 000 particles while still applying the bias potential on the central subsystem of 3000 particles, (iii) storing a configuration of the system every 1000 HMC steps during the equilibration run, and (iv) switching off the bias potential and letting each of these configurations evolve freely during a HMC trajectory[15] at fixed temperature and pressure. We generate 15 HMC trajectories. We observe the dissolution of the nucleus in the surrounding liquid for seven of them and the growth of the nucleus in the remaining eight MD trajectories. The 7:8 ratio, close to the ideal 5:5 ratio, expected for a critical nucleus, demonstrates that the crystal nuclei we have formed are critical nuclei.

10.1021/ja072260n CCC: $37.00

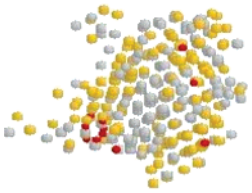

Figure 1. Outside view of a critical nucleus of Al. Gray, fcc; red, bcc; and yellow, hcp.

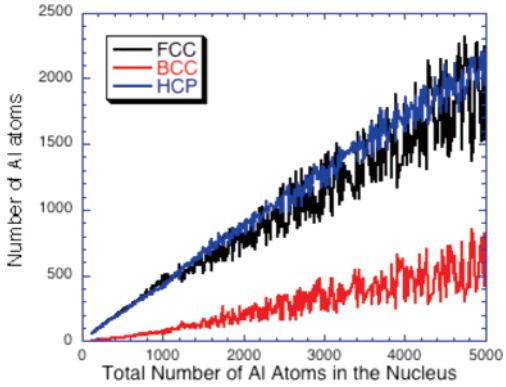

Figure 2. Evolution of the number of fcc, bcc, and hcp atoms as a function of the total number of Al atoms in the nucleus during the growth of the crystal nuclei.

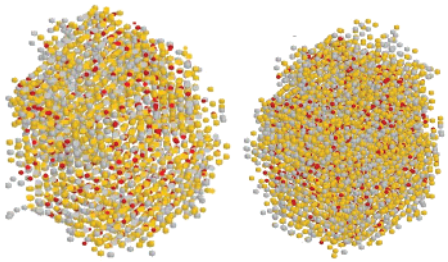

Figure 3. Cross section and outside view of a crystallite obtained after $t = 250$ ps (time $t = 0$ ps indicates the beginning of the growth trajectory). Gray, fcc; red, bcc; and yellow, hcp.

During the growth of the crystal nuclei, we monitor the increases in the number of fcc, hcp, and bcc particles. We present in Figure 2 the averages calculated over all 15 HMC trajectories. Growth proceeds in the same random packing of hcp and fcc phases as observed during the nucleation step. Our analysis confirm that approximately 90% of the Al atoms composing the crystallite are identified as fcc or hcp. The remaining 10% are bcc defects. We did not find any icosahedral signature within the crystallite. We also found that the concentration in icosahedral atoms in the liquid was constant throughout the growth step, showing again that the icosahedral structures do not play an active role in the crystallization process of Al. As shown in Figure 3, the bcc atoms are not restricted to the liquid−solid interface as observed for LJ crystallites. This proves again that bcc does not serve as an intermediate between the solid and the liquid phases for Al.

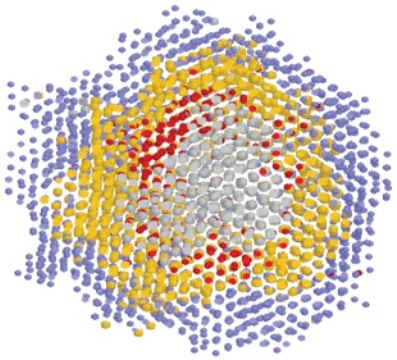

Figure 4. Cross section showing the evolution of a crystal nucleus as a function of time during a growth trajectory. Gray after 20 ps, red after 30 ps, yellow after 40 ps, and blue after 50 ps.

The growth mechanism is presented in Figure 4. Throughout the growth step, Al crystallites remain strongly faceted. Growth does not take place uniformly. As shown in Figure 4, patches of fcc/hcp atoms are successively added to the surface so that the overall shape remains close to a hexagon.

In this communication, we have presented the first molecular simulation of the entire crystallization process of Al, modeled by an accurate many-body (EAM) potential. We have highlighted a number of differences between the pathway to crystallization of Al and that of simple fluids, most likely because of the strong cohesive interactions existing in Al. This suggests that the strategies used to control polymorphism and the crystal morphology during the crystallization of colloids or molecules might not be appropriate for metals.

Supporting Information Available: A detailed description of the simulation methods and parameters as well as the definitions for the local bond order parameters and how we use these parameters to analyze the structure of the crystal nuclei. This material is available free of charge via the Internet at http://pubs.acs.org.

References

(1) Auer, S.; Frenkel, D. *Nature* **2001**, *409*, 1023.
(2) (a) ten Wolde, P. R.; Ruiz-Montero, M. J.; Frenkel, D. *Phys. Rev. Lett.* **1995**, *75*, 2714; *J. Chem. Phys.* **1996**, *104*, 9932. (b) Moroni, D.; ten Wolde, P. R.; Bolhuis, P. G. *Phys. Rev. Lett.* **2005**, *94*, 235703.
(3) Desgranges, C.; Delhommelle, J. *J. Am. Chem. Soc.* **2006**, *128*, 10368.
(4) Desgranges, C.; Delhommelle, J. *J. Am. Chem. Soc.* **2006**, *128*, 15104.
(5) Gasser, U.; Weeks, E. R.; Schofield, A.; Pusey, P. N.; Weitz, D. A. *Science* **2001**, *292*, 258.
(6) Daw, M. S.; Baskes, M. I. *Phys. Rev. Lett.* **1983**, *50*, 1285.
(7) Jasper, N. E.; Schultz, N. E.; Truhlar, D. G. *J. Phys. Chem. B* **2005**, *109*, 3915.
(8) Bath, D.; Jasper, N. E.; Schultz, N. E.; Siepmann, J. I.; Truhlar, D. G. *J. Am. Chem. Soc.* **2006**, *128*, 4224.
(9) Bath, D.; Schultz, N. E.; Jasper, N. E.; Siepmann, J. I.; Truhlar, D. G. *J. Phys. Chem. B* **2006**, *110*, 26135.
(10) Mehlig, B.; Heerman, D. W.; Forrest, B. M. *Phys. Rev. B* **1992**, *45*, 679.
(11) Steinhardt, P. J.; Nelson, D. R.; Ronchetti, M. *Phys. Rev. B* **1983**, *28*, 784.
(12) Alexander, S.; McTague, J. P. *Phys. Rev. Lett.* **1978**, *41*, 702.
(13) Klein, W.; Leyvraz, F. *Phys. Rev. Lett.* **1986**, *57*, 2845.
(14) Frank, F. C. *Proc. R. Soc. London, Ser. A* **1952**, *215*, 43.
(15) Attard, P. *J. Chem. Phys.* **2002**, *116*, 9616.

JA072260N